



# DESIGN AND OPTIMIZATION OF LATTICE STRUCTURES FOR AEROSPACE APPLICATIONS

Enrico Stragiotti

François-Xavier Irisarri<sup>1</sup>, Cédric Julien<sup>1</sup> and Joseph Morlier<sup>2</sup>

1: ONERA - The French Aerospace Lab  
DMAS - Département matériaux et structures  
92320 Châtillon, France  
[{francois-xavier.irisarri, cedric.julien}@onera.fr](mailto:{francois-xavier.irisarri, cedric.julien}@onera.fr)

2: ICA - Institut Clément Ader  
ISAE - SUPAERO  
31400 Toulouse, France  
[joseph.morlier@isae-supraero.fr](mailto:joseph.morlier@isae-supraero.fr)  
December 11, 2023

PhD manuscript

ONERA – ISAE Supaero

## **Colophon**

This document was typeset with the help of KOMA-Script and L<sup>A</sup>T<sub>E</sub>X using the kaobook class.

ONERA – ISAE Supaero

# CONTENTS

<b>Contents</b>	<b>iii</b>
<b>List of Figures</b>	<b>v</b>
<b>List of Tables</b>	<b>v</b>
<b>List of Abbreviations</b>	<b>v</b>
<b>1. Optimizing the layout of the modules in space</b>	<b>1</b>
1.1. Optimize the modules' layout using a modified DMO algorithm . . . . .	1
1.1.1. Definition of the subdomains cross-sectional areas . . . . .	1
1.1.2. Variables penalization schemes . . . . .	1
1.1.3. The optimization formulation and resolution algorithm . . . . .	2
1.1.4. Optimization initialization: a clustering algorithm to identify similarly behaving subdomains . . . . .	5
1.2. Numerical application . . . . .	6
1.2.1. Layout optimization of fixed modules . . . . .	7
1.2.2. Modules and layout optimization . . . . .	9
1.2.3. A benchmark case study: a simply supported modular bridge . . . . .	11
1.2.4. Simply supported 3D beam . . . . .	11
1.3. Conclusion . . . . .	15
<b>Bibliography</b>	<b>17</b>
<b>Appendix</b>	<b>19</b>
<b>A. Sensitivity analysis of the modular structure optimization algorithm</b>	<b>21</b>



## LIST OF FIGURES

1.1.	.....	2
1.2.	.....	3
1.3.	.....	5
1.4.	.....	5
1.5.	Boundary conditions of the 2D cantilever beam divided in $24 \times 12$ subdomains. In the upper part of the image the ground structure of the module composed of $\bar{n} = 6$ elements.	7
1.6.	$V = 832.848$ .....	7
1.7.	$V = 9832.935$ .....	7
1.8.	.....	8
1.9.	.....	9
1.10.	.....	9
1.11.	.....	10
1.12.	.....	10
1.13.	.....	11
1.14.	.....	12
1.15.	.....	13
1.16.	.....	13
1.17.	.....	14

## LIST OF TABLES

1.1.	Material data used for the 2D cantilever beam 2D. ....	7
1.3.	.....	14
1.2.	Material data used for the simply supported 3D beam optimization. ....	15

## LIST OF ABBREVIATIONS

<b>DMO</b>	Discrete Material Optimization
<b>NLP</b>	Non-Linear Programming
<b>RAMP</b>	Rational Approximation of Material Properties



# OPTIMIZING THE LAYOUT OF THE MODULES IN SPACE

# 1

tables always small Introduction

## 1.1. OPTIMIZE THE MODULES' LAYOUT USING A MODIFIED DMO ALGORITHM

The goal is to treat the problem of contemporaneously optimizing the modules' layout and topology of a modular structure. The major scientific challenge is that the layout optimization of the modules in the structure subdomains is a discrete problem, where we can't have intermediate results at the end of the optimization. As we want to use a gradient descent algorithm [1] for this reason we need to find a method to transform a discrete problem into a continuous one.

### 1.1.1. DEFINITION OF THE SUBDOMAINS CROSS-SECTIONAL AREAS

Inspired by the work of Stegmann and Lund on the Discrete Material Optimization (DMO) algorithm [2], we decided here to define the subdomains variables (so the variables of the structure) as a weighted sum of the modules variables. In the case of a ground structure discretized using  $N_{\text{sub}}$  subdomains and  $N_t$  different modules, we define then the cross sectional areas of the subdomain  $j$  as:

$$a^j = \sum_{t=1}^{N_t} w_t^j \bar{a}_t \quad (1.1)$$

where  $\bar{a}_t$  represent the vector of cross sectional areas of the  $t$  module and  $w^j$  is the vector of weight relatives to the  $j$  subdomain, defined as  $w^j \in \mathbb{R}^t \mid w_j^t \in [0, 1]$ .

An example of a cantilever beam with  $N_{\text{sub}} = 8$  and  $N_t = 2$  is given in Fig. 1.1, where we see how the modification of the weight values  $w$  influences the structure topology.

### 1.1.2. VARIABLES PENALIZATION SCHEMES

The limit of the presented approach lies in the fact that at convergence, the weight of every subdomains must be all zero but one to one. This is because intermediate weights would represent a mix of different topologies that would not have mechanical sense and that would prove to be impossible to manufacture. For that reason we implement here an interpolation scheme that penalize intermediate densities. We use here Rational Approximation of Material Properties (RAMP) [3] and not the more used SImp interpolation scheme as RAMP because the derivative it is never infinite nor 0 at zero density.

1.1 OPTIMIZE THE MODULES' LAYOUT USING A MODIFIED DMO ALGORITHM . . . . .	1
1.2 NUMERICAL APPLICATION . . . . .	6
1.3 CONCLUSION . . . . .	15

1. Sigmund (2011), 'On the usefulness of non-gradient approaches in topology optimization'

2. Stegmann et al. (2005), 'Discrete material optimization of general composite shell structures'

3. Stolpe et al. (2001), 'An alternative interpolation scheme for minimum compliance topology optimization'

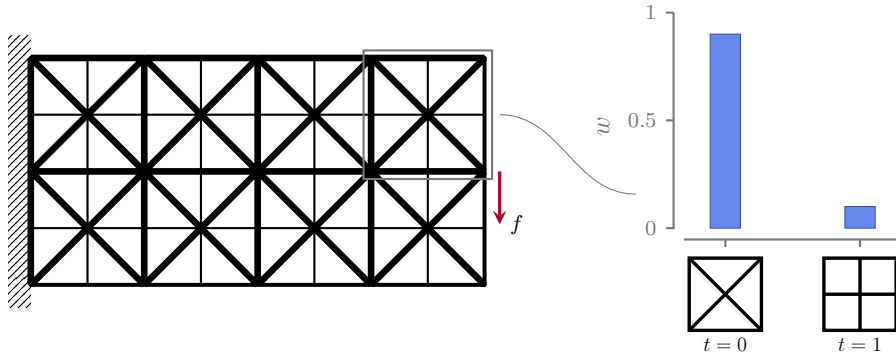


**Figure 1.1.**

We define the design variable  $\alpha$  responsible of the module choice inside of the subdomain  $j$ . its relationship with the weight  $w$  is the following:

$$w_t^j = \frac{\alpha_t^j}{1 + p(1 - \alpha_t^j)} \quad (1.2)$$

where  $p \in \mathbb{R}^+$  is a parameter used to control the steepness of the RAMP interpolation. Additionally, inspired by the works of [4], we put up a multi-phase versions of the RAMP interpolation where we simultaneously penalize mechanical properties and we artificially increase the volume of modules with intermediate densities. To do that we define an additional RAMP parameter, this time always negative  $q \in \mathbb{R}^-$  that is used to evaluate the increased weights associated with the evaluation of the volume  $V$ .

$$V = \sum_{j=1}^{N_{\text{sub}}} \tilde{\boldsymbol{\ell}}^T \tilde{\boldsymbol{a}}^j, \quad (1.3)$$

where  $\tilde{\boldsymbol{a}}$  is defined as following:

$$\tilde{\boldsymbol{a}}^j = \sum_{t=1}^{N_T} \tilde{w}_t^j \bar{\boldsymbol{a}}_t, \quad (1.4)$$

and  $\tilde{w}$

$$\tilde{w}_t^j = \frac{\alpha_t^j}{1 + q(1 - \alpha_t^j)}. \quad (1.5)$$

So for every design variable alpha, we associate two different weights ( $w$  and tilde  $w$ ) that are used to evaluate the mechanical properties and the structure volume, respectively (see Fig. 1.2).

### 1.1.3. THE OPTIMIZATION FORMULATION AND RESOLUTION ALGORITHM

The objective function of the optimization process is the volume minimization of the modular structure. The members of the structure are subject to multiple mechanical constraints, namely stress,

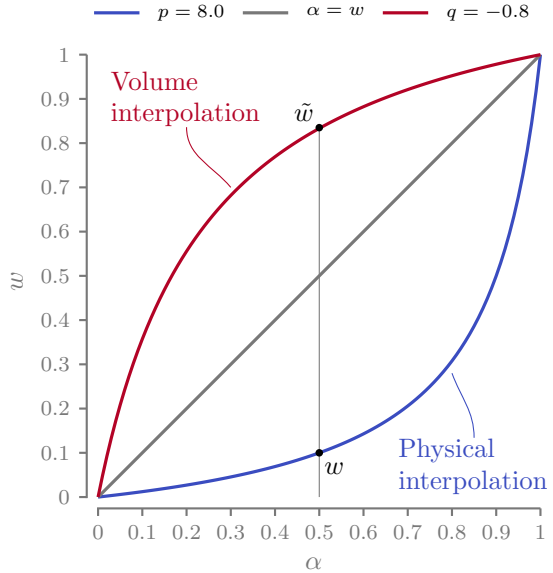


Figure 1.2.

topological buckling, minimum slenderness, and compatibility constraints. Formulation  $M_1$  is stated in terms of modules' cross-sectional area  $\bar{a}$ , module selection variables  $\alpha$ , member forces  $q$  and nodal displacements  $U$  as follows:

$$\begin{aligned}
 & \min_{\bar{a}, \alpha, q, U} \quad V = \sum_{j=1}^{N_{\text{sub}}} \bar{\ell}^T \bar{a}^j \quad (\text{Volume minimization}) \\
 \text{s.t.} \quad & Bq = f \quad (\text{Force equilibrium}) \\
 & q = \frac{aE}{\ell} b^T U \quad (\text{Compatibility constraints}) \\
 & q \geq -\frac{sa^2}{\ell^2} \quad (\text{Euler buckling constraints}) \quad (M_1) \\
 & -\sigma_C a \leq q \leq \sigma_T a \quad (\text{Stress constraints}) \\
 & \bar{a}_{t,r} \geq \bar{a}_{t,r=1} \quad r \in \mathcal{C}_{l,r}(\bar{a}_t), \forall t \\
 & 0 \leq \bar{a} \leq \frac{4\pi\bar{\ell}^2}{\lambda_{\max}} \quad (\text{Slenderness limit}) \\
 & \sum_{t=1}^{N_T} \alpha_t^j \leq 1, \forall j \quad (\text{One selected module max.})
 \end{aligned}$$

This formulation builds on the classic DMO approach, adding multiple mechanical constraints, operating on a ground structure, but most importantly we are not only selecting the best module for every subdomain changing the value of  $\alpha$ , but we are also optimizing the also the modules topology, and all of this at the same time. This is more difficult. The key features of this formulation are essentially the fact that we are dealing with discrete problem and solving it using continuous design variables and a gradient based optimizer. However, we increase considerably the size of the problem, as we are adding numerous additional design variables  $\alpha$  that scales with the number

of subdomains and the number of modules.

The design variable alpha are constrained by a set of constraint that constraint the maximum sum of weights of a j submodule to one. it is important to note that we are treating this constraint as a disequality constraint and not an equality, and for this reason we give the optimizer the ability to put all the weights to zero and remove the subdomain from the structure.

$$\sum_{t=1}^{N_T} \alpha_t^j \leq 1, \forall j \quad (1.6)$$

Problem  $\mathbb{M}_1$  is solved using a modified version of the proposed two step solving algorithm, in which we solve a relaxed problem without compatibility constraints kinematic compatibility constraints are omitted. We call this relaxed Problem  $\mathbb{M}_2$ . this time, as the problem is nonlinear due to the alpha design variables, we solve it without linearizing the buckling constraints. here is the formulation of the first subproblem, formulated in terms of modules' cross-sectional area  $\bar{a}$ , module selection variables  $\alpha$ , member forces  $q$ :

$$\begin{aligned} \min_{\bar{a}, \alpha, q} \quad & V = \sum_{j=1}^{N_{\text{sub}}} \bar{\ell}^T \bar{a}^j \quad (\text{Volume minimization}) \\ \text{s.t.} \quad & Bq = f \quad (\text{Force equilibrium}) \\ & q \geq -\frac{sa^2}{\ell^2} \quad (\text{Euler buckling constraints}) \\ & -\sigma_C a \leq q \leq \sigma_T a \quad (\text{Stress constraints}) \quad (\mathbb{M}_2) \\ & 0 \leq \bar{a} \leq \frac{4\pi\bar{\ell}^2}{\lambda_{\max}} \quad (\text{Slenderness limit}) \\ & \sum_{t=1}^{N_T} \alpha_t^j \leq 1, \forall j \quad (\text{One selected module max.}) \end{aligned}$$

Problem m2 is solved using a gradient based optimizer that exploits iteratively the first and second order derivative to attain convergence. The evaluation of the jacobian and the hessian matrix for this problem is detailed in Appendix A

Once the problem m2 is solved, We fix the module layout on the structure  $\alpha$  and we evaluate the corresponding indexes of the mapping matrix H as follows:

$$h_{j,t} = \begin{cases} 1 & \text{if } \alpha_{j,t} = \max(\alpha_j) \\ 0 & \text{otherwise.} \end{cases} \quad (1.7)$$

Then the compatibility constraints are added again, a FEA is solved to evaluate initial displacements we solve it fixing the submodules

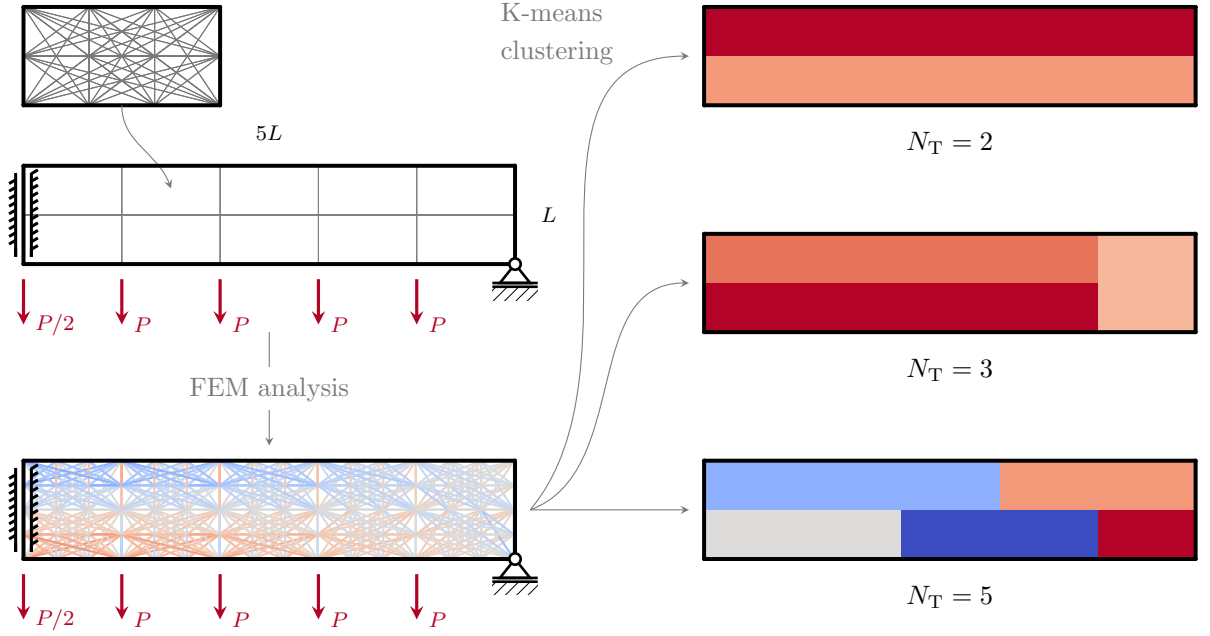


Figure 1.3.

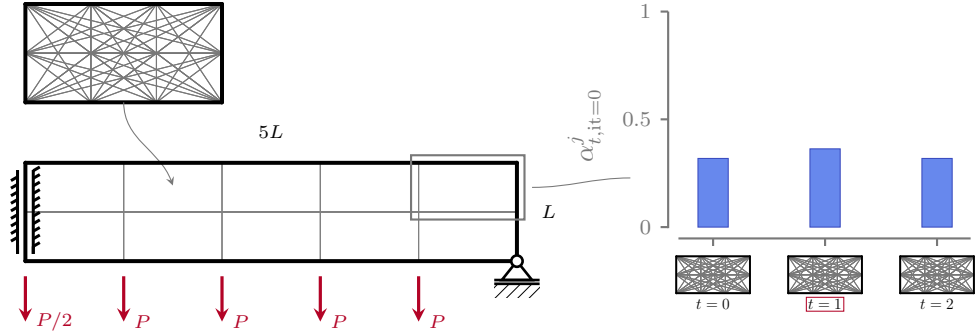


Figure 1.4.

topology and using the VL formulation already used in ... we have no alpha anymore

#### 1.1.4. OPTIMIZATION INITIALIZATION: A CLUSTERING ALGORITHM TO IDENTIFY SIMILARLY BEHAVING SUBDOMAINS

we are not only changing the weights but also the modules topology. the layout is dependent on the module topology and vice versa. It is then really difficult for a gradient based optimizer chose where to go so we give a slightly influenced departure point  $x_0$ . In this work we decided to influence the weight distribution as follows:

$$\alpha_{t,it=0}^j = \begin{cases} \frac{1}{N_T} \cdot 1.1 & \text{if the } j\text{-th subdomain has the } t\text{-th module selected,} \\ \frac{N_T-1.1}{N_T(N_T-1)} & \text{otherwise.} \end{cases} \quad (1.8)$$

the initial layout of modules is assessed using a k-means clustering technique with  $N_T$  clusters. Given a set of observations  $(x_1, x_2, \dots,$

Formulation  $\mathbb{M}_1$  permits to optimize modular structures with fixed module layout. It is stated in terms of modular cross-sectional areas  $\bar{a}$ , member forces  $q$  and nodal displacements  $U$  as follows:

$$\begin{aligned} \min_{\bar{a}, q, U} \quad & V = \ell^T a \\ \text{s.t.} \quad & a = \sum_{t=1}^{N_T} h_t \otimes \bar{a}_t \\ & Bq = f \\ & q = \frac{aE}{\ell} b^T U \\ & q \geq -\frac{sa^2}{\ell^{*2}} \\ & -\sigma_c a \leq q \leq \sigma_t a \\ & \bar{a}_{t,r} \geq \bar{a}_{t,r=1} \\ & 0 \leq \bar{a} \leq \frac{4\pi\ell^2}{\lambda_{\max}}, \end{aligned}$$

$xn$ ), where each observation is a d-dimensional real vector, k-means clustering aims to partition the n observations into n sets. we define the observation as the vector containing the FEA calculated stress distribuition on the uniform initial ground structure. Additionally we add the stress state S For the j-th submodule we define the

$$S^j = \sum_{i=0}^{\bar{n}} |\sigma_i^j| \quad (1.9)$$

This add permits to promote the clustering of not only submodules loaded in similar ways, but also on similar magnitude (and have so more voluminous and less voluminous modules). the full process is depicted in Fig. 1.3, where we see how differently the clustering is conducted starting from the same starting point (the FEA calculated stress distribuition on the uniform initial ground structure) but with different number of clusters (2,3, and 5). Fig. 1.4 finally shows the initial starting point of the optimization, with uniform initialization of  $\bar{a}$  and the biased weight distribution based on the k means clustering.

## 1.2. NUMERICAL APPLICATION

All of the examples presented in this section are solved using the proposed two step formulation, where in the first step we solve a relaxed formulation (no compatibility constraints) to find the optimized modules layout and topology. later, the layout of the modules is fixed, and we solve the optimization problem again to force the structure to comply with the compatibility constraints. The formulations are solved using the non liner interior point solver IPOPT for the two optimization steps

A continuation scheme is set up on the penalization parameter  $q$  of the RAMp interpolation scheme used to evaluate the subdomain volume, where the parameter is set up at zero, and then it increase to -0.4 and -0.8 every time the (and the optimizer is not in a restoration phase). The continuaion scgheme is implemented only on  $q$  as IPOPT is an interior point algorithm, and increasing the  $p$  parameter would put the optimizer well outside of the fesable region everi time the parameter every time it is increased, creating a less than ideal situation

The stopping criterion used for the Non-Linear Programming (NLP) optimizations is  $\|\Delta_{NLP}\|_\infty \leq tol_{nlp}$ , with and  $tol_{nlp} = 10^{-8}$ .  $\Delta_{NLP}$  represents the scaled NLP error, a more comprehensive value used by IPOPT to take into account the optimality of the solution and the constraints violation. The objective function is always scaled so that the initial volume is 1000, the areas are in the interval [0, 100], the initial forces in [0, 100], and the displacement in [0, 100] for the NLP. Several additional parameters are used in the NLP step for cyipopt and IPOPT:

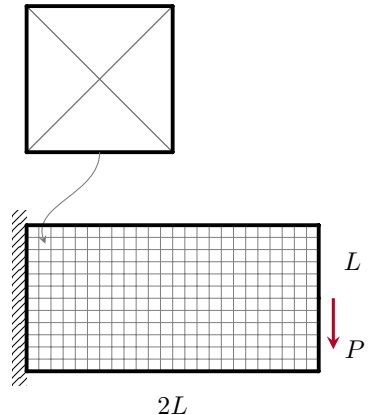
- ▶ `mu_strategy` is set to `adaptive`
- ▶ `jac_c_constant` is set to `yes`
- ▶ `num_linear_variables` is set to `N`, with `N` equal to the number of bars as the force is linear in this problem
- ▶ `grad_f_constant` is set to `yes`
- ▶ `linear_solver` is set to `pardiso`
- ▶ `bound_push` is set to `1e-12`
- ▶ `constr_viol_tol` is set to `1e-6`
- ▶ `nlp_scaling_method` is set to `user-scaling`.

### 1.2.1. LAYOUT OPTIMIZATION OF FIXED MODULES

The proposed formulation is very versatile and permits to solve very different optimization problem. We start now by optimizing the most simple we can for modular structures. We want to optimize the distribution of a fixed topology cell inside a given domain, and the optimizer should only chose between having the subdomain populated or not. We take a single module topology that is held fixed during the optimization, so  $nt=1$  and  $\bar{a}_i = 0.6$ ,  $\forall i$ . The only degree of freedom given to the optimizer is the value of the weight  $w$  controlled by the design variable  $\alpha$ .

The structure that is optimized is a two dimensional cantilever beam of dimension  $200 \times 100$  with a center load of magnitude  $P = 1$ . The optimization domain is partitioned into  $24 \times 12$  submodules on the  $x$  and  $y$  axis, respectively. Every subdomain is populated with a simple fully connected  $2 \times 2$  nodes ground structure as shown in Fig. 1.5. The units of the test case are normalized and a list of the geometry and material parameters is given in Table 1.1. Additionally, in these examples buckling and compatibility constraints are relaxed for simplicity and to preserve the solution simmetry.

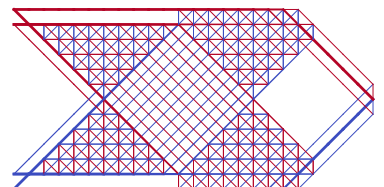
Before showing and commenting the optimization results, we presents two extreme cases that allow us to better understand and put into perspective the optimization results. first, we set up a monolithic optimization with no modular constraints and setting a maximum cross sectional area  $a_{\max} = 0.6$ . The optimization is performed on the same ground structure shown in Fig. 1.5. This results shold represent the lower bound of the optimization, representing the minimum value at which modular optimization should tend, the closer to this value, the better. The resulting topology shows a volume  $V = 832.848$  and a thopology that ressembles the one that are obtained in classic topology optimization. Secondly, a we present a fully modular structure, in which all the subdomains presrnt the topology of the fixed topology module with all bars set to 0.6. In that case the structure shows a volume  $V = 9832.935$  and it represent the upper bound for the optimization. The topology of the fully modular structure is shown in Fig. 1.7.



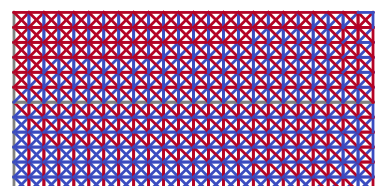
**Figure 1.5.:** Boundary conditions of the 2D cantilever beam divided in  $24 \times 12$  subdomains. In the upper part of the image the ground structure of the module composed of  $\bar{n} = 6$  elements.

Parameter	Value
$L$	100
$\sigma_c, \sigma_t$	$\pm 1$
$P$	1
$a_{\max}$	0.6

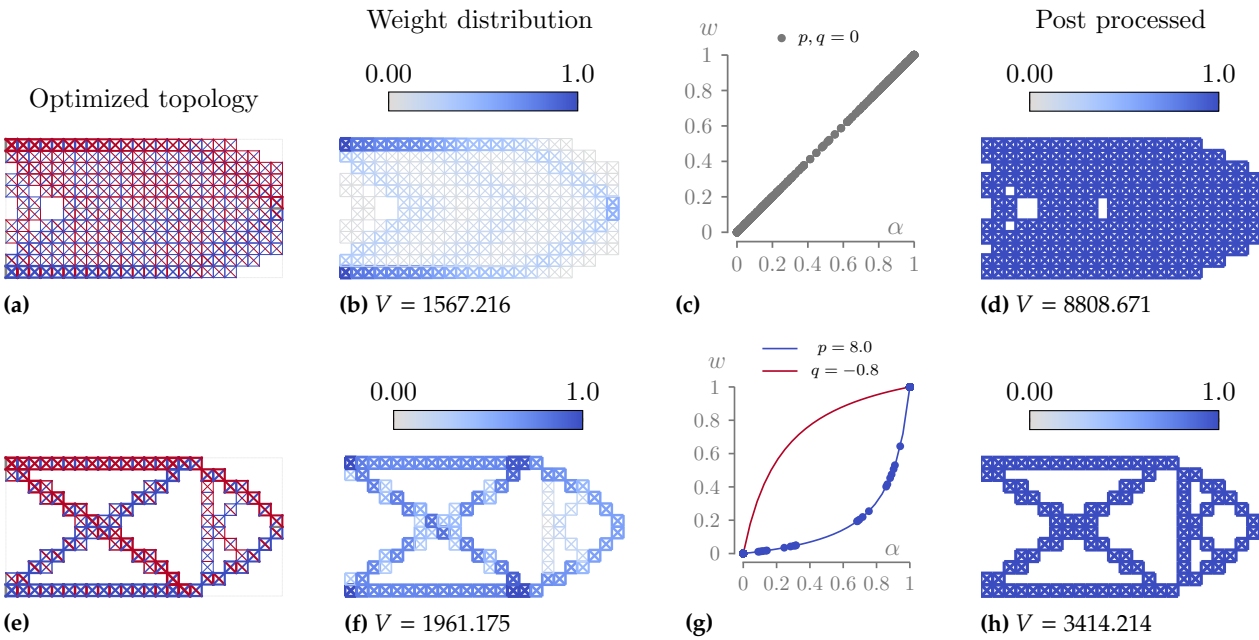
**Table 1.1.:** Material data used for the 2D cantilever beam 2D.



**Figure 1.6.:**  $V = 832.848$



**Figure 1.7.:**  $V = 9832.935$

**Figure 1.8.**

Now that we have set up the reference for better understand the optimization results, we perform the optimizations of the layout of the fixed topology module. Just for the first example we decided not to penalize intermediate weights, so  $p = q = 0$  and then  $w = \alpha$ . The optimized structure topology is shown in Fig. 1.8a and Fig. 1.8b, in which we show also the weight distribution of the solution. At this stage, the optimized structure shows a volume  $V = 1567.216$ , a value that is not that far from the monolithic reference. However, this solution is non physical as many subdomains present intermediate weights and we need to threshold the result. The thresholding value is set to 0.01, so any subdomains that have a weight  $w$  less than this value is considered empty. The result of the thresholding is presented in Fig. 1.8d, in which we see that all weights are now set to 1. The resulting structure has a volume  $V = 8808.671$ , a very noticeable increase due to the high number of intermediate weights shown by the solution of Fig. 1.8b.

add frase on ramp curve

To solve this problem, we set up a multi-phase RAMP interpolation where we simultaneously penalize mechanical properties (using the parameter  $p$ ) and we artificially increase the volume (using the parameter  $q$ ) of modules with intermediate weights. In this optimization we set  $p = 8$  and  $q_{\min} = -0.8$ , and a continuation scheme is used on the  $q$  parameter to gradually decrease it to the minimum value as already explained in Section 1.2. The optimized structure topology with penalized intermediate weights is shown in Fig. 1.8e and Fig. 1.8f and it has a volume  $V = 1961.175$ , a 25 % volume increase with respect

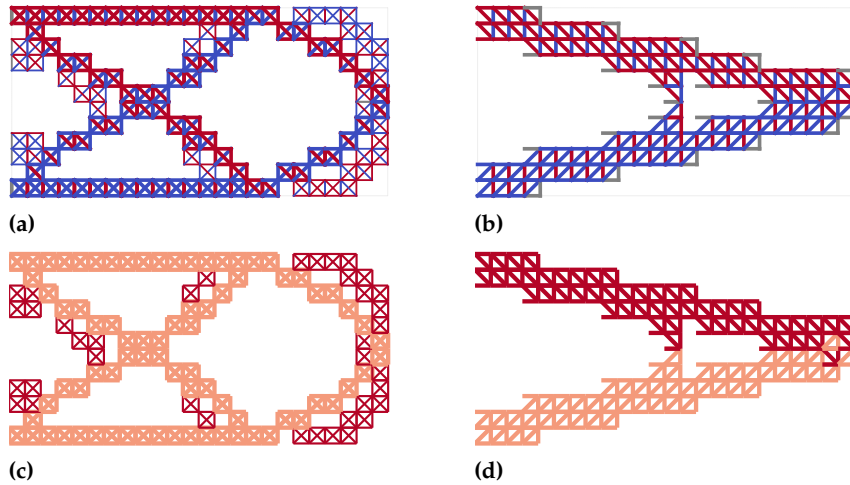


Figure 1.9.

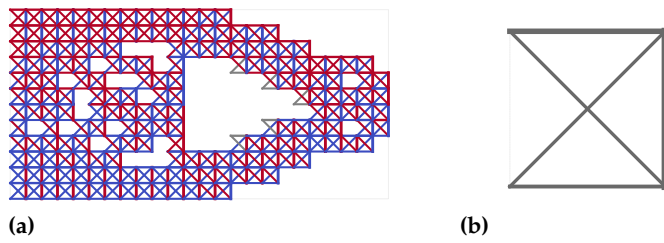


Figure 1.10.

to the unpenalized structure. however we can clearly see how this solution present way less subdomains with intermediate weight and this is very reflected after the thresolding phase, in wich the volume is now  $V =$ , more than 60 % less than the unpenalized structure. the difference between the structure of fig and fig could also be less , as in this case we see that the subdomains creates beams tat are made by only an elements and it is enough to transfer the loads. a finer subdivision of the initial structure could then beneficial.

Similarities with classic topology optimization. [5, 6]

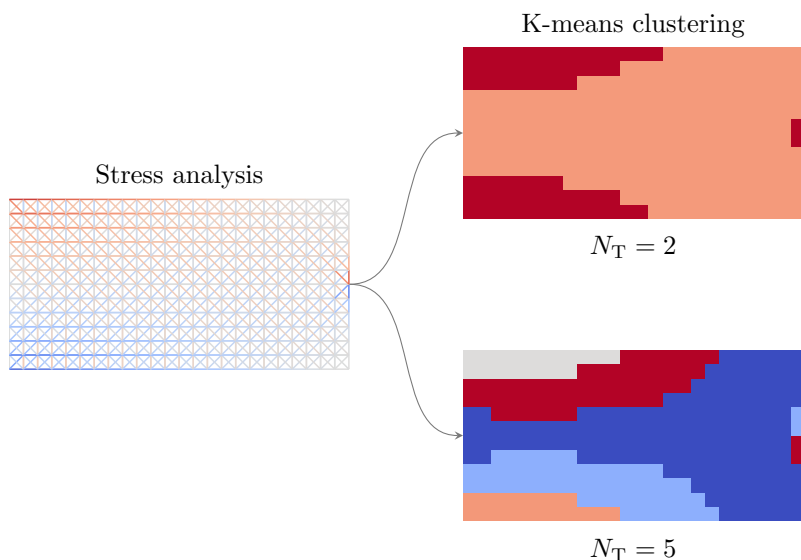
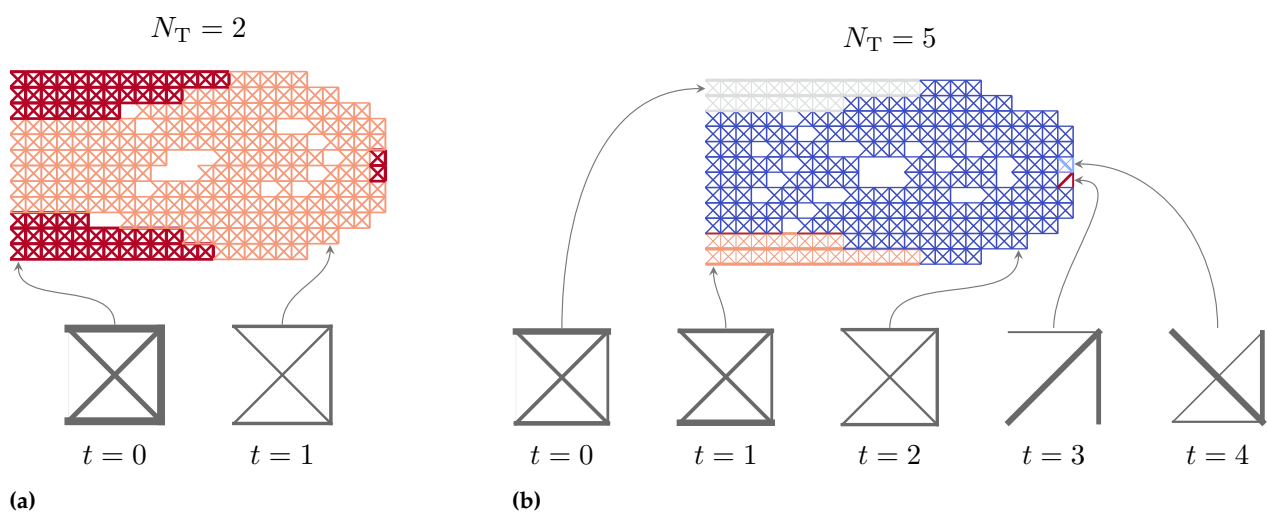
An additional test we performed was to . In these two test cases no perturbation is done on the initial starting point and alpha at iteration 0 is set to  $\alpha = 0.5, \forall j, t$

5. Bendsøe et al. (1999), 'Material interpolation schemes in topology optimization'

6. Sigmund et al. (2016), 'On the (non-)optimality of Michell structures'

### 1.2.2. MODULES AND LAYOUT OPTIMIZATION

tables with volume and phi and psi for different NT

**Figure 1.11.****Figure 1.12.**

### 1.2.3. A BENCHMARK CASE STUDY: A SIMPLY SUPPORTED MODULAR BRIDGE

difference with tugilimana, we take into account the buckling when solving the first subproblem of module layout, we can have an empty subdomain and we use a gradeint descent algo

principalmente due motivi, cambia il metodo di rottura, non più buckling e poi ho i vuoti

### 1.2.4. SIMPLY SUPPORTED 3D BEAM

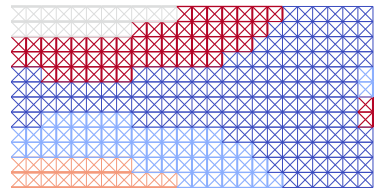
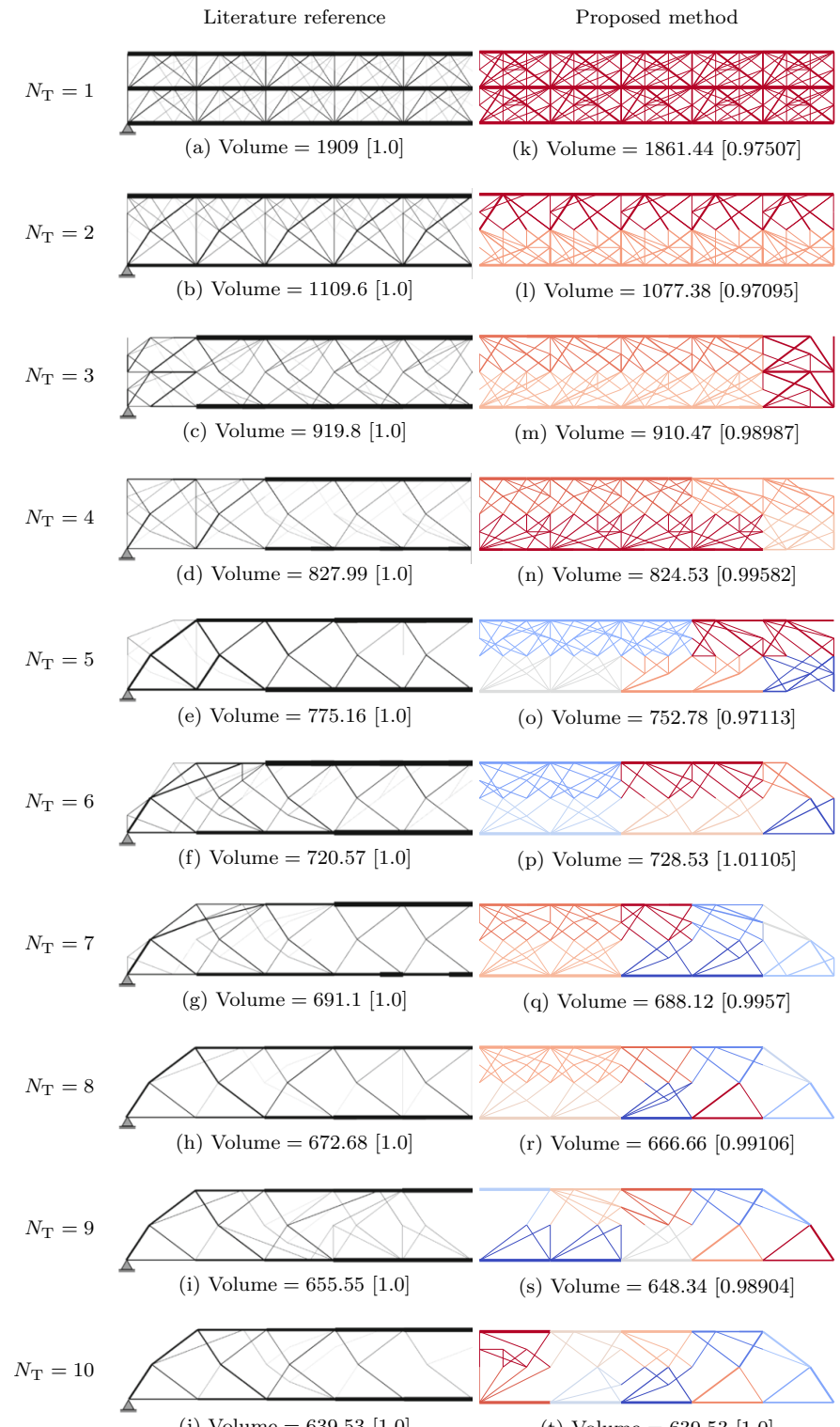


Figure 1.13.

**Figure 1.14.**

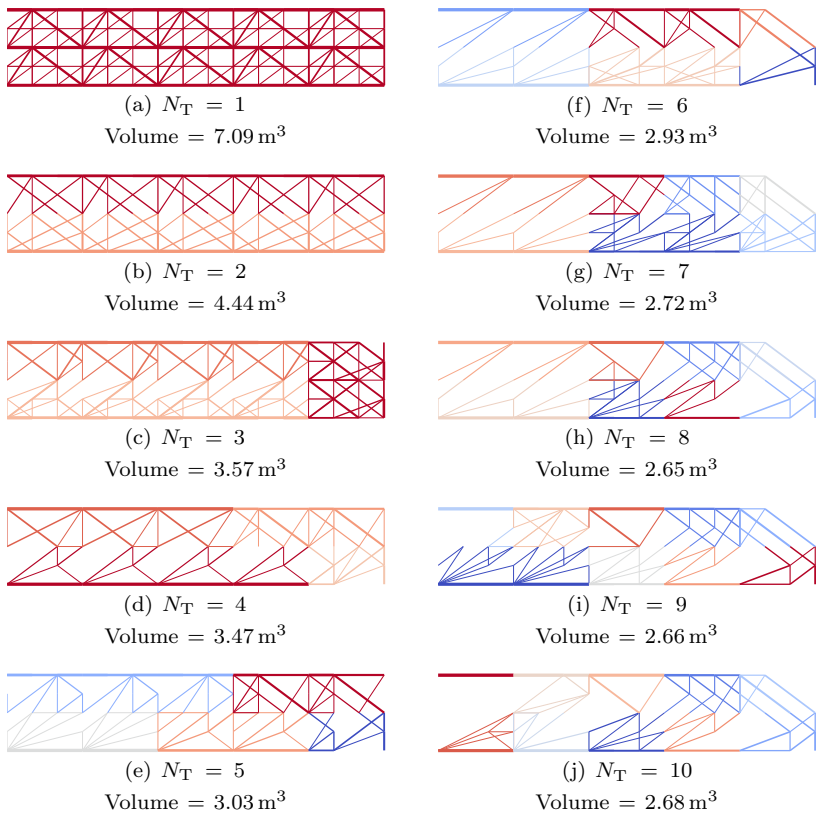


Figure 1.15.

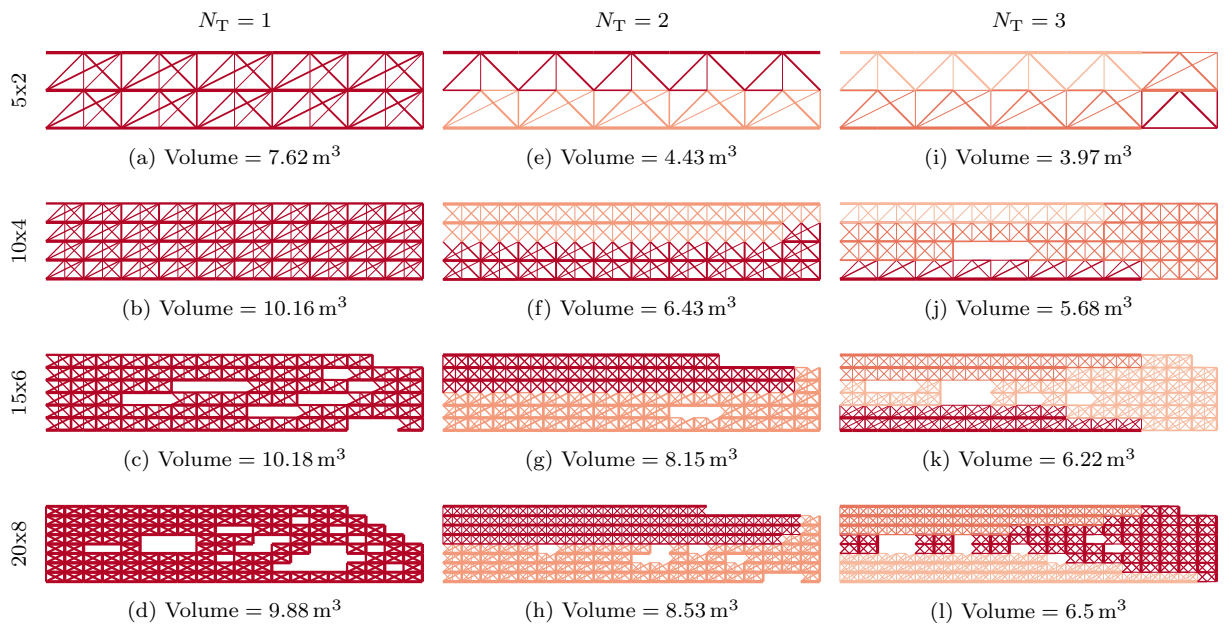
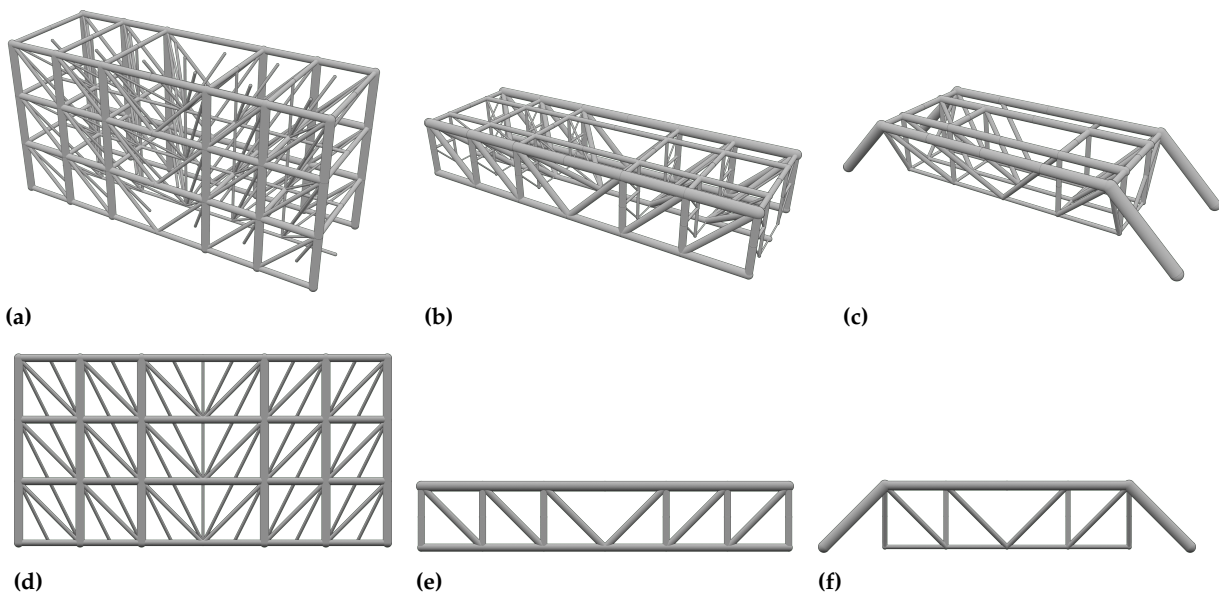


Figure 1.16.

**Table 1.3.**

$N_T$	-	1	2	3
$N_{\text{sub}}$	1	36	36	36
$N_{\text{opt}} (N_{\text{el}})$	20 (1984)	360 (12636)	204 (12636)	104 (12636)
$V [\text{cm}^3]$	9.907	27.958	15.548	10.178
$V [\%]$	1.761	4.970	2.764	1.809
$\bar{\rho} [\text{kg/m}^3]$	80.31	226.65	126.05	82.51
$C [\text{J}]$	3.71	5.20	6.21	4.141
$a_{\text{max}} [\text{mm}^2]$	37.61	9.40	12.81	15.81
$\varphi$	100.00 %	21.11 %	39.21 %	80.77 %
$\psi$	1.00	0.47	0.66	0.87
$t$	4 s	1 m 18 s	42 s	10 m 22 s

**Figure 1.17.**

### 1.3. CONCLUSION

Parameter	Value
$E$	2.7 GPa
$\nu$	0.3
$\sigma_c, \sigma_t$	$\pm 55$ MPa
$\rho$	$1.14 \text{ g cm}^{-3}$
$P$	100 N

**Table 1.2.:** Material data used for the simply supported 3D beam optimization.



## BIBLIOGRAPHY

- [1] Sigmund, Ole, 'On the usefulness of non-gradient approaches in topology optimization', *Structural and Multidisciplinary Optimization* 43.5 (May 2011), pp. 589–596.  
DOI: [10.1007/s00158-011-0638-7](https://doi.org/10.1007/s00158-011-0638-7) cited on page 1
- [2] Stegmann, J. and Lund, E., 'Discrete material optimization of general composite shell structures', *International Journal for Numerical Methods in Engineering* 62.14 (Apr. 2005), pp. 2009–2027.  
DOI: [10.1002/nme.1259](https://doi.org/10.1002/nme.1259) cited on page 1
- [3] Stolpe, M. and Svanberg, K., 'An alternative interpolation scheme for minimum compliance topology optimization', *Structural and Multidisciplinary Optimization* 22.2 (Sept. 2001), pp. 116–124.  
DOI: [10.1007/s001580100129](https://doi.org/10.1007/s001580100129) cited on page 1
- [4] Hvejsel, Christian Frier and Lund, Erik, 'Material interpolation schemes for unified topology and multi-material optimization', *Structural and Multidisciplinary Optimization* 43.6 (June 2011), pp. 811–825.  
DOI: [10.1007/s00158-011-0625-z](https://doi.org/10.1007/s00158-011-0625-z) cited on page 2
- [5] Bendsøe, M. P. and Sigmund, O., 'Material interpolation schemes in topology optimization', *Archive of Applied Mechanics* 69.9 (Nov. 1999), pp. 635–654.  
DOI: [10.1007/s004190050248](https://doi.org/10.1007/s004190050248) cited on page 9
- [6] Sigmund, Ole, Aage, Niels, and Andreassen, Erik, 'On the (non-)optimality of Michell structures', *Structural and Multidisciplinary Optimization* 54.2 (Aug. 2016), pp. 361–373.  
DOI: [10.1007/s00158-016-1420-7](https://doi.org/10.1007/s00158-016-1420-7) cited on page 9



## **APPENDIX**



# SENSITIVITY ANALYSIS OF THE MODULAR STRUCTURE OPTIMIZATION ALGORITHM

A

## SENSITIVITY ANALYSIS

### COMMON DERIVATIVES

$$\frac{\partial \mathbf{a}^j}{\partial \bar{\mathbf{a}}_t} = w_t^j \quad (\text{A.1})$$

$$\frac{\partial \mathbf{a}^j}{\partial \alpha_t^j} = \frac{\partial \mathbf{a}^j}{\partial w_t^j} \frac{\partial w_t^j}{\partial \alpha_t^j} \quad (\text{A.2})$$

$$\frac{\partial \mathbf{a}^j}{\partial w_t^j} = \bar{\mathbf{a}}_t \quad (\text{A.3})$$

$$\frac{\partial w_t^j}{\partial \alpha_t^j} = \frac{1 + (\cdot)}{(1 + (\cdot))(1 - \alpha_t^j)^2} \quad (\text{A.4})$$

where  $(\cdot)$  is either equal to  $p$  or  $q$ .

$$\frac{\partial^2 w_t^j}{\partial (\alpha_t^j)^2} = \frac{2(\cdot)(1 + (\cdot))}{(1 + (\cdot))(1 - \alpha_t^j)^3} \quad (\text{A.5})$$

### VOLUME JACOBIAN

$$\frac{\partial V}{\partial \bar{\mathbf{a}}_t} = \bar{\ell}^T \sum_{j=1}^{N_{\text{sub}}} \tilde{w}_t^j, \text{ with } t \in [1, \dots, N_T] \quad (\text{A.6})$$

$$\frac{\partial V}{\partial \alpha_t^j} = \frac{\partial V}{\partial w_t^j} \frac{\partial w_t^j}{\partial \alpha_t^j} \quad (\text{A.7})$$

$$\frac{\partial V}{\partial w_t^j} = \bar{\ell}^T \bar{\mathbf{a}}_t \quad (\text{A.8})$$

$$\frac{\partial V}{\partial q} = 0 \quad (\text{A.9})$$

$$\frac{\partial V}{\partial U} = 0 \quad (\text{A.10})$$

**VOLUME HESSIAN**

$$\frac{\partial^2 V}{\partial \bar{a}_t \partial \alpha_t^j} = \bar{\ell}^T \frac{\partial \tilde{w}_t^j}{\partial \alpha_t^j} \quad (\text{A.11})$$

$$\frac{\partial^2 V}{\partial (\alpha_t^j)^2} = \bar{\ell}^T \bar{a}_t \frac{\partial^2 w_t^j}{\partial (\alpha_t^j)^2} \quad (\text{A.12})$$

$$\frac{\partial^2 V}{\partial \bar{a}_t^2} = 0 \quad (\text{A.13})$$

**EQUILIBRIUM JACOBIAN**

$$g_{\text{eq}} := Bq = f \quad (\text{A.14})$$

Not impacted by the clustering of the variables.

$$\frac{\partial g_{\text{eq}}}{\partial \alpha} = 0 \quad (\text{A.15})$$

**STRESS CONSTRAINTS TENSION JACOBIAN**

$$g_t := q - \sigma_t a \leq 0 \quad (\text{A.16})$$

$$\frac{\partial g_t^j}{\partial \bar{a}_t} = \frac{\partial g_t^j}{\partial a^j} \frac{\partial a^j}{\partial \bar{a}_t} \quad (\text{A.17})$$

$$\frac{\partial g_t^j}{\partial a^j} = -\sigma_t \quad (\text{A.18})$$

$$\frac{\partial g_t^j}{\partial \bar{a}_t} = -\sigma_t w_t^j \quad (\text{A.19})$$

$$\frac{\partial g_t^j}{\partial \alpha^j} = \frac{\partial g_t^j}{\partial a^j} \frac{\partial a^j}{\partial \alpha^j} \quad (\text{A.20})$$

**STRESS CONSTRAINTS TENSION HESSIAN**

$$\frac{\partial^2 g_t^j}{\partial \bar{a}_t \partial \alpha_t^j} = -\sigma_t \frac{\partial w_t^j}{\partial \alpha_t^j} \quad (\text{A.21})$$

$$\frac{\partial^2 g_t^j}{\partial (\alpha_t^j)^2} = -\sigma_t \bar{a}_t \frac{\partial^2 w_t^j}{\partial (\alpha_t^j)^2} \quad (\text{A.22})$$

**BUCKLING JACOBIAN**

$$g_b := q \frac{s \mathbf{a}^2}{\ell^2} \geq 0 \quad (\text{A.23})$$

$$\frac{\partial g_b^j}{\partial \mathbf{a}^j} = 2 \frac{s \mathbf{a}^j}{\ell^2} \quad (\text{A.24})$$

$$\frac{\partial g_b^j}{\partial \bar{\mathbf{a}}_t} = \frac{\partial g_b^j}{\partial \mathbf{a}^j} \frac{\partial \mathbf{a}^j}{\partial \bar{\mathbf{a}}_t} \quad (\text{A.25})$$

$$\frac{\partial g_b^j}{\partial \bar{\mathbf{a}}_t} = 2 \frac{s \mathbf{a}^j}{\ell^2} w_t^j \quad (\text{A.26})$$

$$\frac{\partial g_b^j}{\partial \alpha^j} = \frac{\partial g_b^j}{\partial \mathbf{a}^j} \frac{\partial \mathbf{a}^j}{\partial \alpha^j} \quad (\text{A.27})$$

$$\frac{\partial g_b^j}{\partial \alpha_t^j} = 2 \frac{s \mathbf{a}^j}{\ell^2} \bar{\mathbf{a}}_t \frac{\partial w_t^j}{\partial \alpha_t^j} \quad (\text{A.28})$$

$$\frac{\partial g_b^j}{\partial \alpha_t^j} = 2 \frac{s \mathbf{a}^j}{\ell^2} \bar{\mathbf{a}}_t \frac{1 + (\cdot)}{\left(1 + (\cdot)(1 - \alpha_t^j)\right)^2} \quad (\text{A.29})$$

**BUCKLING HESSIAN**

$$\frac{\partial^2 g_b^j}{\partial \bar{\mathbf{a}}_l \partial \alpha_m^j} = 2 \frac{s}{\ell^2} w_l^j \frac{\partial \mathbf{a}^j}{\partial \alpha_m^j} + 2 \frac{s \mathbf{a}^j}{\ell^2} \frac{\partial w_l^j}{\partial \alpha_m^j} \quad (\text{A.30})$$

$$\frac{\partial^2 g_b^j}{\partial \bar{\mathbf{a}}_l \partial \alpha_m^j} = 2 \frac{s}{\ell^2} w_l^j \frac{\partial w_m^j}{\partial \alpha_m^j} \bar{\mathbf{a}}_m + 2 \frac{s \mathbf{a}^j}{\ell^2} \frac{\partial w_l^j}{\partial \alpha_m^j} \quad (\text{A.31})$$

$$\frac{\partial^2 g_b^j}{\partial \bar{\mathbf{a}}_l \partial \alpha_m^j} = \begin{cases} 2 \frac{s}{\ell^2} \frac{\partial w_l^j}{\partial \alpha_t^j} \left( w_t^j \bar{\mathbf{a}}_t + \mathbf{a}^j \right) & \text{if } l = m = t \\ 2 \frac{s}{\ell^2} w_l^j \frac{\partial w_m^j}{\partial \alpha_m^j} \bar{\mathbf{a}}_m & \text{otherwise.} \end{cases} \quad (\text{A.32})$$

$$\frac{\partial^2 g_b^j}{\partial \bar{\mathbf{a}}_l \partial \bar{\mathbf{a}}_m} = 2 \frac{s}{\ell^2} w_l^j w_m^j \quad (\text{A.33})$$

$$\frac{\partial^2 g_b^j}{\partial \alpha_l^j \partial \alpha_m^j} = 2 \frac{s}{\ell^2} \bar{\mathbf{a}}_l \frac{\partial \mathbf{a}^j}{\partial \alpha_m^j} \frac{\partial w_l^j}{\partial \alpha_l^j} + 2 \frac{s \mathbf{a}^j}{\ell^2} \bar{\mathbf{a}}_l \frac{\partial^2 w_l^j}{\partial \alpha_l^j \partial \alpha_m^j} \quad (\text{A.34})$$

$$\frac{\partial^2 \mathbf{g}_b^j}{\partial \alpha_l^j \partial \alpha_m^j} = \begin{cases} 2 \frac{s}{t^2} \bar{\mathbf{a}}_t^2 \left( \frac{\partial w_t^j}{\partial \alpha_t^j} \right)^2 + 2 \frac{s a_t^j}{t^2} \bar{\mathbf{a}}_t \frac{\partial^2 w_t^j}{\partial (\alpha_t^j)^2} & \text{if } l = m = t \\ 2 \frac{s}{t^2} \bar{\mathbf{a}}_l \bar{\mathbf{a}}_m \left( \frac{\partial w_m^j}{\partial \alpha_m^j} \right) \left( \frac{\partial w_l^j}{\partial \alpha_l^j} \right) & \text{otherwise.} \end{cases} \quad (\text{A.35})$$